Talanta 126 (2014) 20–26

Contents lists available at ScienceDirect

Talanta

journal homepage: www.elsevier.com/locate/talanta

A novel functionalisation process for glucose oxidase immobilisation in poly(methyl methacrylate) microchannels in a flow system for amperometric determinations

Marcos Rodrigues Facchini Cerqueira [a,b], Daniel Grasseschi [b], Renato Camargo Matos [a], Lucio Angnes [b,*]

[a] Departamento de Química, Universidade Federal de Juiz de Fora (UFJF), Juiz de Fora, MG 36036-900, Brazil
[b] Universidade de São Paulo, Instituto de Química, Avenida Professor Lineu Prestes, 748, São Paulo, SP CEP 05508-000, Brazil

ARTICLE INFO

Article history:
Received 22 December 2013
Received in revised form
18 February 2014
Accepted 19 February 2014
Available online 24 March 2014

Keywords:
Poly(methyl methacrylate)
Microreactor
Glucose oxidase
Glucose
Amperometry

ABSTRACT

Different materials like glass, silicon and poly(methyl methacrylate) (PMMA) are being used to immobilise enzymes in microchannels. PMMA shows advantages such as its low price, biocompatibility and attractive mechanical and chemical properties. Despite this, the introduction of reactive functional groups on PMMA is still problematic, either because of the complex chemistry or extended reaction time involved. In this paper, a new methodology was developed to immobilise glucose oxidase (GOx) in PMMA microchannels, with the benefit of a rapid immobilisation process and a very simple route. The new procedure involves only two steps, based on the reaction of 5.0% (w/w) polyethyleneimine (PEI) with PMMA in a dimethyl sulphoxide medium, followed by the immobilisation of glucose oxidase using a solution containing 100 U enzymes and 1.0% (v/v) glutaraldehyde. The reactors prepared in this way were evaluated by a flowing system with amperometric detection (+0.60 V) based on the oxidation of the H_2O_2 produced by the reactor. The microreactor proposed here was able to work with high bioconversion and a frequency of 60 samples h^{-1}, with detection and quantification limits of 0.50 and 1.66 μmol L^{-1}, respectively. Michaelis–Menten parameters (V_{max} and K_M) were calculated as 449 ± 47.7 nmol min^{-1} and 7.79 ± 0.98 mmol. Statistical evaluations were done to validate the proposed methodology. The content of glucose in natural and commercial coconut water samples was evaluated using the developed method. Comparison with spectrophotometric measurements showed that both methodologies have a very good correlation ($t_{calculated,\ 0.05,\ 4} = 1.35 < t_{tabled,\ 0.05,\ 4} = 2.78$).

1. Introduction

Microfluidic devices have received considerable attention from researchers in recent years. Since the early 1990s, when Manz et al. [1] developed the first microfluidic device, these systems have become more popular as a result of their advantages over larger scale systems. Among these, their small dimensions, large surface-to-volume ratio, well-defined reaction times and small sample quantities requirements make these systems very promising with regard to their use for analytical procedures [2–4].

In this context, the use of microchannels for enzymatic applications has also gained support. Different materials like glass [5], polystyrene [6], silicon [7,8] and poly(methyl methacrylate) (PMMA) [9], have already been used to immobilise enzymes. PMMA shows some advantages compared to other materials, such as its low price, biocompatibility, excellent optical transparency and attractive mechanical and chemical properties [10].

The most common way to immobilise enzymes onto a microreactor is by using a support that can covalently attach to the enzyme or by a cross-linking agent, which can act as a spacer-arm molecule [11]. Immobilisation of enzymes provides many advantages such as their reuse, lower consumption of reagents and samples, higher analysis rate, extended lifetime and greater stability. However, for this purpose, the substrate of the reactor must have some reactive functional groups that can interact with the enzymes. A few approaches have already been made to introduce amino groups onto PMMA sheets [12–14].

Amino groups are well-known functional groups for enzyme immobilisation, but these modifications require long reaction times and/or the consumption of a large amount of reagents. The method most commonly used to add amine functionality to the surface of PMMA is a reaction with a lithiated diamine [14], but this reaction is air sensitive and the lithiated amines have limited lifetimes. In this context, Brown et al. [15] found a faster way to

* Corresponding author. Tel.: +55 11 3091 3828; fax: +55 11 3091 3781.
E-mail address: luangnes@iq.usp.br (L. Angnes).

http://dx.doi.org/10.1016/j.talanta.2014.02.048
0039-9140/

react PMMA with NH_2 groups. In their study, an ethylenediamine solution in dimethyl sulphoxide (DMSO) solvent was used and yielded 2-fold more amino groups on PMMA surface, when compared to other methodologies. The use of different amino reactants can also enhance the number of amino groups on PMMA surface. Bai et al. [16] observed that polyethyleneimine (PEI) gave the highest number of amino groups on PMMA due to its higher density of amino groups on the polymeric surface area after modification, resulting in a greater number of binding sites. Another advantage that can be associated with the use of PEI in relation to other amino groups containing reactants is the creation of a suitable microenvironment for enzyme immobilisation, improving its stability [17].

In this work, a rapid and very efficient process for GOx immobilisation on PMMA microreactors is described. In comparison with a previous study presented by our group [9], the new process requires less time and enhances the enzymatic immobilisation rate. This is based on PMMA functionalisation with PEI (using DMSO as solvent), followed by GOx immobilisation on the microchannel walls, using glutaraldehyde as the cross-linking agent. The performance of the enzymatic reactor prepared in this way was evaluated for glucose by differential amperometric determinations.

2. Material and methods

2.1. Reagents and solutions

All reagents were of analytical grade. Sodium dihydrogen phosphate, sodium hydrogen phosphate and isopropyl alcohol were purchased from Synth (Diadema, Brazil). Glutaraldehyde 25% and D-(+)-glucose were purchased from Merck (Darmstadt, Germany). Polyethyleneimine (MW 750,000, 50% in water), dimethyl sulphoxide and 4-aminoantipyrine were acquired from Sigma-Aldrich (St. Louis, MO, USA). Glucose oxidase from *Aspergillus niger* (124 U mg^{-1}) was purchased from Toyobo (Osaka, Japan) and horseradish peroxidase (115 U mg^{-1}) from Seppim (Puteaux, France).

Solutions were prepared with deionised water obtained from a Milli-Q water purification system (Dubuque, IA, USA). The resistivity measured after this treatment was not less than 18.2 MΩ cm. Coconut water samples were purchased from a local store. Four bottled coconut water samples, some of them extracted directly from the fruit, were evaluated.

2.2. Microchannel manufacture

Laser ablation has been widely employed to fabricate PMMA microdevices [18]. In this process, the beam of a high-energy laser is used to break bonds in polymer molecules and remove the decomposed fragments from the ablated regions [10].

In order to engrave PMMA plates with microchannels, a CO_2 laser-engraving machine (L-Solution 100, from Gravograph Industry International La Chapelle-St Luc, France) was used. The microchannel design was made using Corel Draw 12 software (Corel Corporation-version 12.0.0.458-2003). Engravings with 500 μm width, 200 μm depth and different lengths were crafted into an 8.5 cm × 5.5 cm × 2.0 mm PMMA plate. Reactors with 61.5 cm length were utilised for the majority of the measurements.

After digging the microchannel, the PMMA plate was washed with deionised water, dried, and then thermally sealed onto a 2.0 mm thick PMMA plate with the same dimensions. The sealing process was carried out using a heat press (model HT3020) operated at 110 °C under 590 kPa for 30 min.

2.3. Flow system and electrochemical configuration

The main constituents of the proposed method are depicted in Fig. 1. The flow arrangement was composed of two distinct propelling systems: an aquarium pump (A) was utilised to pneumatically propel the carrier electrolyte [19], and a programmable peristaltic pump (D) (Reglo MS Digital, Ismatec), used to introduce reproducible sample volumes into the microchannel (F). Injection of samples by the peristaltic pump was performed using 0.3 mm internal diameter Tygon® tubing. A throttle (B), located between the electrolyte reservoir and the pneumatic pump, allowed control of the flow rate into the microchannels.

Electrochemical measurements were performed using a μ-Autolab type III potentiostat (EcoChemie, Netherlands) in the chronoamperometric mode. Hydrogen peroxide (H_2O_2) generated by the microreactor was detected using a three-electrode system. A commercial dual platinum electrode (G_1) was employed as working and counter-electrodes and a miniaturised $Ag/AgCl_{(sat)}$ (G_4) was used as the reference electrode. A thin polypropylene layer (200 μm thickness—G_2) was used as a spacer to limit the electrochemical cells bound. A PMMA cover (G_3) was used to seal the cell. This seal was fixed using four screws located at the edges of the structure. In addition, three holes were drilled on the top of the PMMA cover. Two of them were used as the input and output of the flowing solution. The connections were made with 0.3 mm i.d. Tygon® tubing. The third hole was made exactly in front of the working electrode as a way to adapt the miniaturised $Ag/AgCl_{(sat)}$ reference electrode [20].

The arrangement depicted in Fig. 1 was explored to determine the kinetics parameters of the immobilised enzymes and to quantify glucose in coconut water samples. All samples were diluted in 0.10 mol L^{-1} phosphate buffer solution (pH 7.0) just before each analysis. Sample dilutions ranged from 1:100 to 1:2000.

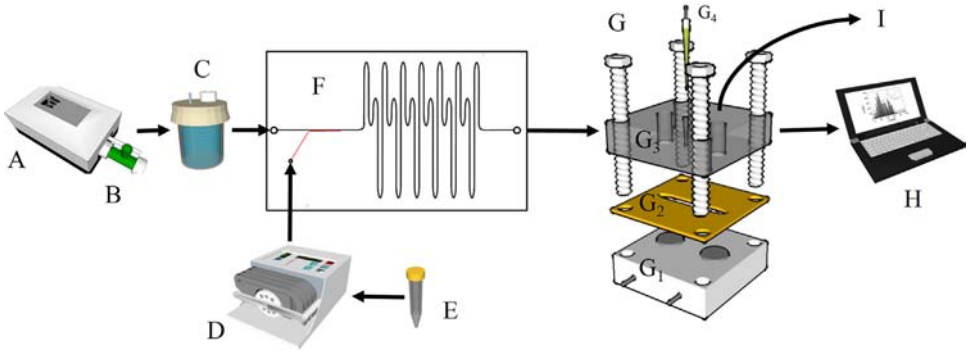

Fig. 1. Configuration of the applied micro flow system: (A) one-way pneumatic propellant aquarium pump, (B) throttle, (C) electrolyte reservoir, (D) programmable peristaltic pump, (E) sample, (F) microreactor, (G) electrochemical cell, (G_1) commercial dual platinum electrode, (G_2) polypropylene layer (200 μm thickness), (G_3) PMMA cover with holes, (G_4) miniaturised $Ag/AgCl_{(sat)}$ electrode, (H) microcomputer and (I) waste.

2.4. Microchannel modification and characterisation

Microchannel modifications were made based on the procedure described by Brown et al. [15], except for the usage of PEI, instead of ethylenediamine, as the source of NH_2 groups.

All microchannel modifications were made after the sealing step, under flowing conditions. This procedure is advantageous, as it prevents enzymatic denaturation during the hot sealing process and additionally contributes to optimise the modification route. Flow rates of 15 μL min^{-1} and 150 μL min^{-1} were used during the modification and cleaning step, respectively. These flow rates were used to guarantee greater contact between the PMMA surface and the reactants during the modification process, and to reproduce the analysis conditions during microchannel cleaning.

To perform the microchannel modification, it was initially cleaned by flowing isopropanol for 5 min in order to remove any impurities that could be attached to the channel walls. A 5.0% (w/w) PEI solution in DMSO (a SN_2 promoting organic solvent) was then passed through the microchannel for 20 min. In sequence, the microchannel was dried under an N_2 stream and excess PEI was removed with a 0.10 mol L^{-1} phosphate buffer solution (pH 7.0), flowing for 5 min. The flow rate used here was the same as that used in the cleaning process. 5 mL of a freshly prepared mixture of GOx (100 U) and glutaraldehyde 1.0% (v/v) in phosphate buffer solution was then flowed through the microchannels for 35 min. Finally, the microchannels were washed again with phosphate buffer solution (5 min) and dried with an N_2 stream. Fig. 2 schematically shows the reactions for GOx immobilisation.

The functionalised surfaces were characterised by Raman spectroscopy measurements, performed with a WITec confocal Raman microscope model Alpha 300R equipped with Ar, Nd:YAD and He–Ne lasers. The presented spectra were acquired with the excitation laser operating at 532 nm.

2.5. Spectrophotometric measurements

In order to evaluate the precision of the proposed method, parallel spectrophotometric determination of glucose was also carried out utilising a well-established method [21], utilising a mixture of 5.0 mmol L^{-1} phenol, 0.50 mmol L^{-1} 4-aminoantipyrine, 15 U mL^{-1} GOx and 20 U mL^{-1} peroxidase, all in 0.10 mol L^{-1} phosphate buffer (pH 7.0). After dilution, solutions were kept for 1 h (at room temperature), to enable the reaction to take place. Measurements were carried out using a quartz cell with a 1.00 cm optical path at 500 nm using a spectrophotometer 600 Plus (Femto, Brazil).

3. Results and discussion

3.1. Microchannel characterisation

Fig. 3 shows a set of Raman spectra after each step in the immobilisation process. Fig. 3A shows typical Raman bands achieved for pristine PMMA [22]. PEI modification on the surface, after PMMA treatment with DMSO, can be confirmed mainly by

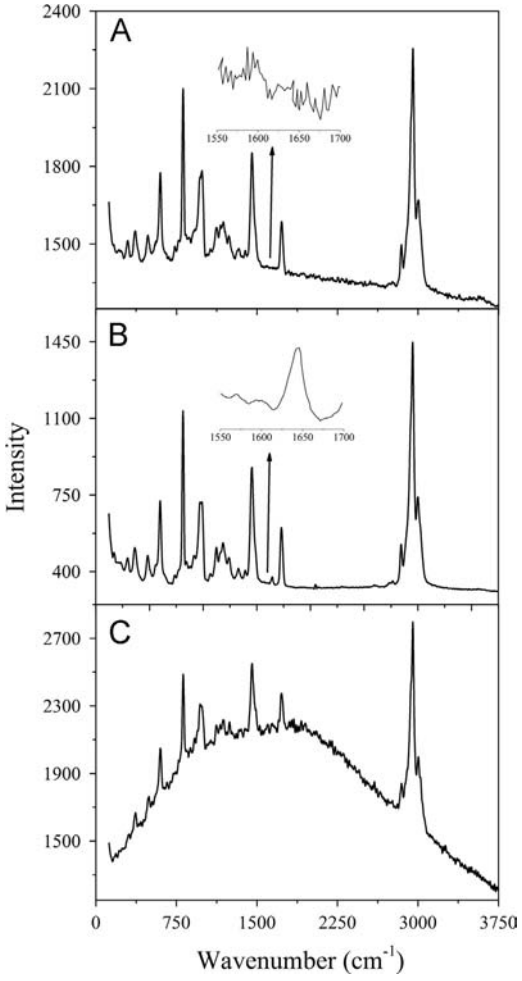

Fig. 3. Raman spectra of clean pristine PMMA microchannels (A) and after treatment with PEI (B) and glutaraldehyde (C).

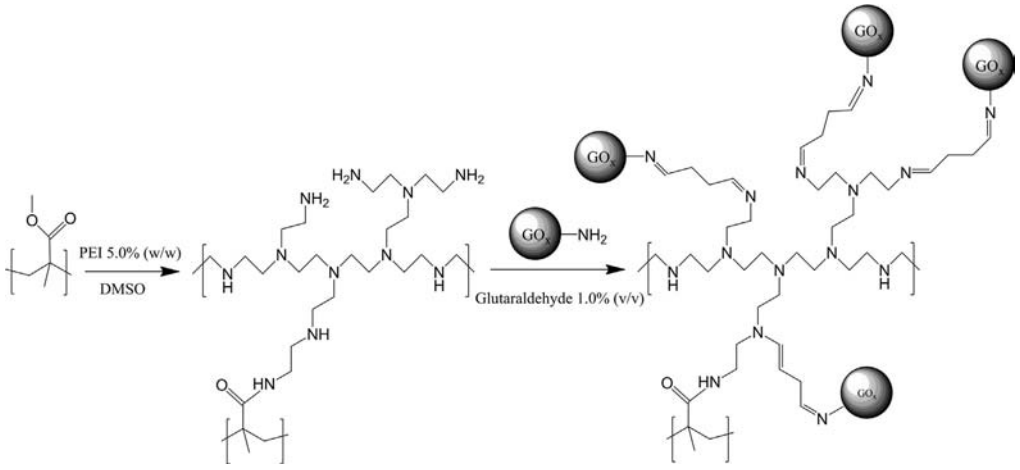

Fig. 2. The schematic route for glucose immobilisation on PMMA microchannels.

the presence of an NH_2 bending band ($\approx 1640\ cm^{-1}$) in the respective Raman spectrum (Fig. 3B). The small amount of reacted PEI on the microchannel surface leads to low intensity bands upon Raman spectroscopy and, for this reason, other bands that could be assigned to PEI were not measured. After glutaraldehyde addition, the high number of –C═N– bonds (as indicated in Fig. 2) leads to high fluorescence after Raman excitation (Fig. 3C). Raman measurements after GOx immobilisation were ineffective since only an increase in the measured fluorescence over the previous step could be observed (spectra not shown). This increase may be caused by the highly fluorescent chromophore flavin, belonging to flavin-adenine dinucleotide (FAD), which is responsible for the redox activity of GOx [9], or to the increase in the number of –C═N– bonds.

In order to demonstrate the effectiveness of the enzymatic immobilisation, the following experiments were done in two distinct reactors—one with immobilised GOx and another without the enzyme. The same mixture used in the colorimetric measurements, with the exception of GOx (5.0 mmol L^{-1} phenol, 0.50 mmol L^{-1} 4-aminoantipyrine, 20 U mL^{-1} peroxidase, and 0.10 mol L^{-1} phosphate buffer), in the presence of 10.0 mmol L^{-1} glucose was introduced. Fig. 4 shows the difference in the colour developed in the reactor containing immobilised GOx (Fig. 4B), by injecting the solution described above (Fig. 4A). In the reactor without immobilised enzymes, after 1 h, any colour was developed (Fig. 4C).

3.2. Flow system evaluation

The developed system was evaluated towards its application for amperometric determination of glucose. Parameters of the applied flow system such as carrier flow-rate, injected samples volumes and microchannel length were evaluated. The analytical response for the studied range of each parameter is presented in Fig. 5.

The analytical signal usually increases linearly with higher injected volumes. However, a loss in linearity is observed when the dispersion of sample in the carrier stream starts to decrease (higher injected volumes). Injected volumes ranging from 2.5 μL to 17.5 μL were evaluated, as shown in Fig. 5A. A linear increase in the current signal was observed until an injected volume of 10.0 μL was reached, while higher values showed a non-linear increase. For this reason, this sample volume (10 μL) was applied for the following measurements.

Lower flow rates (Fig. 5B) were found to give higher current signals since more glucose is converted into H_2O_2, due to a longer residence time. However, it also affected the analytical frequency of the method, as it can be seen by the sample rate decrease (b_1=110 samples h^{-1}, b_2=90 samples h^{-1}, b_3=70 samples h^{-1}, and b_4=45 samples h^{-1}). This parameter is crucial if lower detection limits are required [23]. The flow rate adopted (150 μL min^{-1}) was selected considering simultaneous sensibility and analytical frequency.

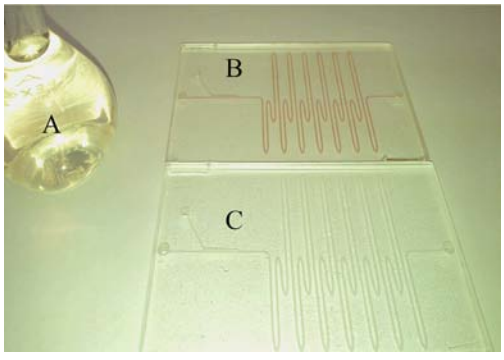

Fig. 4. Image of a colorimetric test made to confirm the immobilisation of GOx on the PMMA microchannel, using the solution (A) described in Section 3.1.

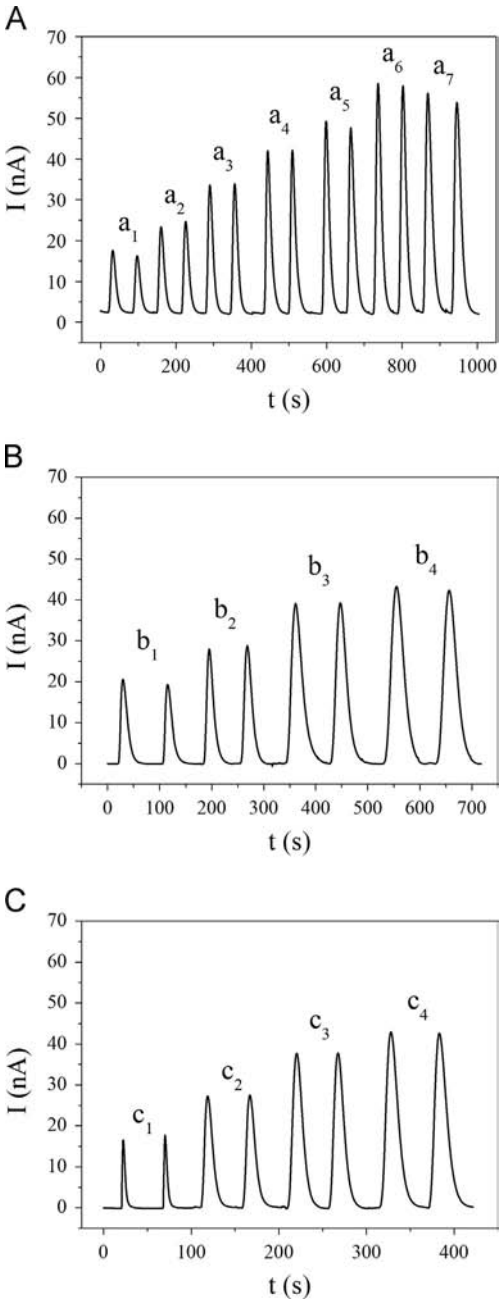

Fig. 5. Effect of flow parameters on amperometric response of a 0.10 mmol L^{-1} glucose standard solution: (A) injected volume (a_1: 2.50 μL, a_2: 5.00 μL, a_3: 7.50 μL, a_4: 10.0 μL, a_5: 12.5 μL, a_6: 15.0 μL and a_7: 17.5 μL), (B) flow rate (b_1: ~300 μL min^{-1}, b_2:~200 μL min^{-1}, b_3: ~150 μL min^{-1} and b_4: ~85 μL min^{-1}) and (C) microchannel length (c_1: 13.0 cm, c_2: 32.5 cm, c_3: 44.5 cm and c_4: 61.5 cm). For each experiment, conditions were fixed as follow: (A) flow rate of ~200 μL min^{-1} and microchannel length of 61.5 cm, (B) injected volume of 10.0 μL and microchannel length of 61.5 cm and (C) injected volume of 10.0 μL and flow rate of ~200 μL min^{-1}.

Longer microchannels led to higher current signals. Despite the fact that a longer course implies higher sample dispersion, it also enables a greater number of immobilisation sites, resulting in an increase in the bioconversion rate (Fig. 5C). In the same way that it affects samples dispersion, enlarging the microchannel path also affects the analytical frequency, as sample rate is decreased (c_1=327 samples h^{-1}, c_2=120 samples h^{-1}, c_3=100 samples h^{-1}, and c_4=80 samples h^{-1}). A 61.5 cm microchannel was chosen to

achieve significant signal and also good analytical frequency. Longer channels were not evaluated, since a loss in system throughput, in relation to the rate of analysis, was not desired.

3.3. Kinetic study

Adopting the optimal values obtained above, kinetic studies were developed, aiming to evaluate the microreactor efficiency. The catalytic conversion of a substrate (S) and co-substrate (O_2), by means of an oxidase enzyme (E) with FAD as prosthetic group, to produce a product (P), can be written as [24]

$$S + E(FAD) \rightarrow P + E(FADH_2) \quad (1)$$

$$E(FADH_2) + O_2 \rightarrow E(FAD) + H_2O_2 \quad (2)$$

The two-substrate form of the Michaelis–Menten equation for the overall reaction rate (V) is given by [24]

$$V = \frac{V_{max}}{1 + K_M(S)/[S] + K_M(O_2)/O_2} \quad (3)$$

where V_{max} is the maximum reaction rate of the system and K_M is defined as the concentration of substrate that gives half V_{max}. Both values are known as Michaelis–Menten parameters and are a good way to determine the efficiency of enzymatic biotransformation.

However, if the co-substrate concentration is constant and higher than the substrate concentration, which is often the case, Eq. (3) can be written as [24]

$$V = \frac{V_{max}}{1 + K_M(S)/[S]} \quad (4)$$

Eq. (4) describes the rate of H_2O_2 production on the microreactor, which is lately detected on the electrode surface. As glucose standards are introduced in the microreactor, a certain amount of H_2O_2 is produced, depending on V_{max} and K_M values. The current measured after each glucose addition is proportional to the concentration of the generated H_2O_2

$$I = k[H_2O_2]_{generated} \quad (5)$$

However, when applying flow systems, the kinetics parameters of the microreactor depend directly on the applied flow rate (as it affects the contact time of the substrate and the enzyme), since it is usually much higher than the dispersion coefficient in solution. The overall reaction rate can thus be given by [25]

$$V = [H_2O_2]_{generated}\Phi \quad (6)$$

where Φ is the system flow rate. When the operating conditions are modified, either by alternating the proportion of the reactants or changing the flow rate, the conversion rate of the reactor changes [26].

As the amount of produced H_2O_2 is unknown, and since the parameters involved in "k" term of Eq. (5) are hard to determine, a calibration plot, ranging from 1.0 μmol L^{-1} to 10.0 mmol L^{-1} (I (μA) = 0.083(±0.002) + 1.370(±0.031) [H_2O_2] (mmol L^{-1}), R^2: 0.995), was constructed for generated H_2O_2 quantification (data not shown).

In order to determine the kinetic parameters and the linearity response range of the proposed immobilisation procedure, a glucose concentration study situated between 5.0 μmol L^{-1} and 50.0 mmol L^{-1} was performed (Fig. 6A). The signals obtained demonstrated a linear response from 5.00 μmol L^{-1} to 2.00 mmol L^{-1} (I (μA) = 0.006(±0.003) + 0.502(±0.007) [Glucose] (mmol L^{-1}), R^2: 0.999) (Fig. 6B).

Within the values found for the H_2O_2 produced (by means of H_2O_2 and glucose calibration plots), the reaction rate was defined as a function of the flow rate (150 μL min^{-1}). Since values higher than 10.0 mmol L^{-1} led to non-increasing current signals (Fig. 6A and B), probably due to saturation of enzyme sites, an increased competition of glucose and H_2O_2 towards the electrode active sites (since glucose standards are highly concentrated), or even because of solution viscosity enhancement, they were not considered for kinetics parameters evaluation. Fig. 7 shows the correlation of the glucose standard concentration and reaction rate.

V_{max} and K_M values were calculated by using a nonlinear least fitting square (with weighting factors) to directly fit the experimental data from Eq. (4). Values are equal to 449 ± 47.7 nmol min^{-1} (V_{max}) and 7.79 ± 0.98 mmol (K_M), where K_M is in accordance with values found by random PEI/GOx immobilisation [27]. This value shows the good stability of the developed microreactor, since lower values of K_M show that the enzyme achieves its maximum catalytic efficiency at low substrate concentrations.

The activity of surface enzyme towards glucose was also evaluated by means of its efficiency. O'Neill et al. proposed a way to normalise the biosensor response with respect to H_2O_2 sensitivity, by using the slopes of the biosensor response for H_2O_2 solutions and for the H_2O_2 produced by the biosensor [24]. Slopes of both calibration plots were used to calculate the bioreactor efficiency by

$$E\,(\%) = \text{Slope}\,(S) \times 100/\text{Slope}\,(H_2O_2) \quad (7)$$

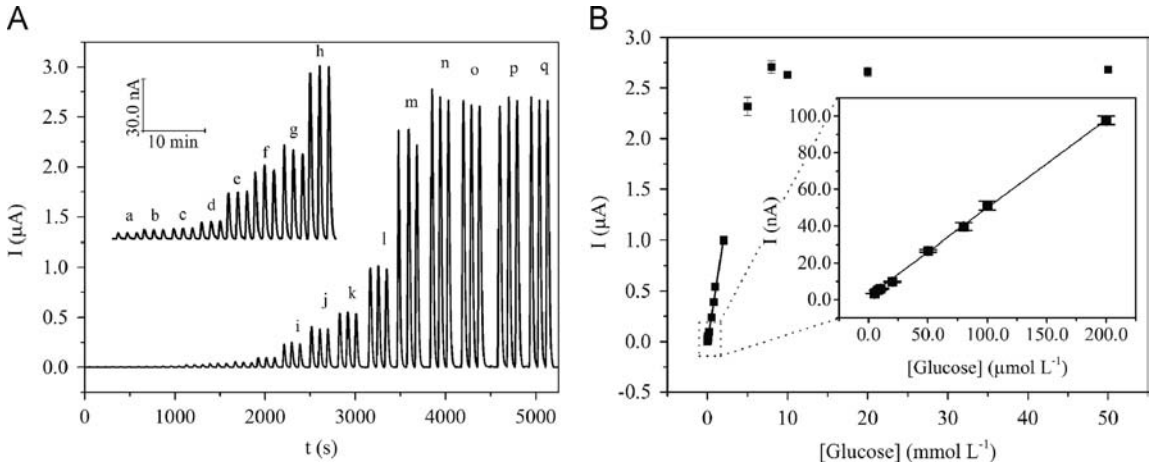

Fig. 6. (A) Diagram for evaluation of the system linearity through the described range (a: 5.00 μmol L^{-1}, b: 8.00 μmol L^{-1}, c: 10.0 μmol L^{-1}, d: 20.0 μmol L^{-1}, e: 50.0 μmol L^{-1}, f: 80.0 μmol L^{-1}, g: 100 μmol L^{-1}, h: 200 μmol L^{-1}, i: 500 μmol L^{-1}, j: 800 μmol L^{-1}, k: 1.00 mmol L^{-1}, l: 2.00 mmol L^{-1}, m: 5.00 mmol L^{-1}, n: 8.00 mmol L^{-1}, o- 10.0 mmol L^{-1}, p: 20.0 mmol L^{-1} and q: 50.0 mmol L^{-1}) and (B) linearity through the studied range in (A). Records were made using +0.60 V vs. $Ag/AgCl_{(sat)}$. 0.10 mol L^{-1} phosphate buffer (pH 7.0) was used as a carrier solution. Other conditions are listed in Section 3.2.

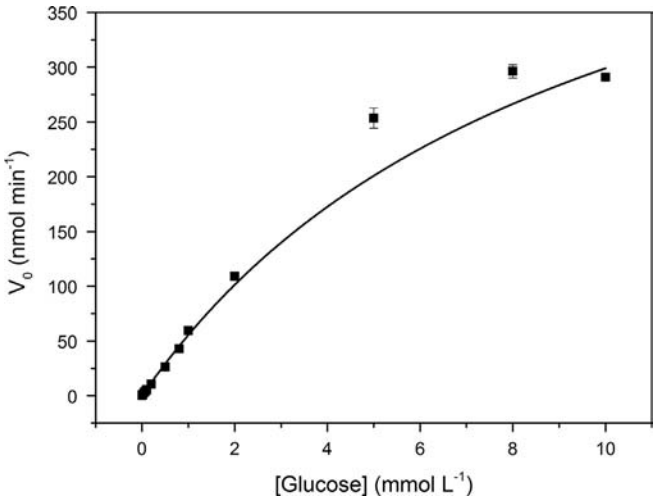

Fig. 7. Michaelis–Menten fitting of bioreaction rate over glucose standard concentration.

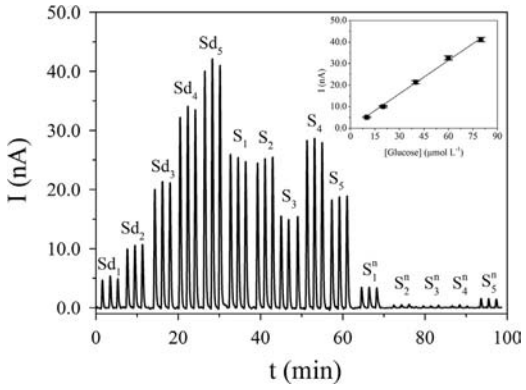

Fig. 8. Analysis of glucose in coconut water. Calibration plot: (Sd_1) 10.0 μmol L^{-1}, (Sd_2) 20.0 μmol L^{-1}, (Sd_3) 40.0 μmol L^{-1}, (Sd_4) 60.0 μmol L^{-1}, and (Sd_5) 80.0 μmol L^{-1}. S_1–S_5 and S_1^n–S_5^n refer to the passage of samples through the microreactor with and without immobilised GOx, respectively. Measurement conditions were the same used in Fig. 6.

A value of 36.6% of bioconversion was found, utilising the conditions adopted in this work. It is important to notice that if higher values of conversion are required, a simple decrease in the system flow rate can be implemented.

3.4. Microchannel performance towards glucose determination

Standard deviation (s.d.) of the lowest detectable standard (1 μmol L^{-1}) was applied for measuring detection (3.3 times s.d.) and quantification (10 times s.d.) limits of the method, with obtained values of 0.50 μmol L^{-1} and 1.66 μmol L^{-1}, respectively.

To verify the repeatability of the proposed method, 105 injections of glucose (0.10 mmol L^{-1}) were performed. The analysis of this series of measurements gave an average current value of 40.1 nA and a relative standard deviation (RSD) of 3.81%. The analytical frequency obtained was 60 samples h^{-1}. To evaluate the durability of the microreactor, 1200 injections of glucose (0.10 mmol L^{-1}) were made in a single reactor, over a period of one week. During this period, the microreactor was used, washed with phosphate buffer solution, dried with an N_2 flow and stored in a refrigerator at 4 °C. After this period, the current signal decreased to about 50.0% of its initial signal. Several factors may have contributed to the decrease in signal, such as the decrease in enzyme activity.

Table 1
Result for analysis of five different coconut water samples by the proposed and spectrophotometric methods.

Samples	Amperometry		Spectrophotometry (UV–vis)	
	[Glucose] (mmol L^{-1})	R.S.D. (%)	[Glucose] (mmol L^{-1})	R.S.D. (%)
S_1 (natural)	4.28	2.28	5.13	2.74
S_2	96.08	2.41	93.77	1.75
S_3	28.79	1.99	31.29	3.92
S_4	109.43	1.35	124.68	0.38
S_5	33.12	2.38	34.66	0.54

3.5. Quantification of glucose in coconut water samples

Coconut water samples were analysed without any pre-treatment. The samples were diluted directly in 0.10 mol L^{-1} phosphate buffer (pH 7.0) and injected into the microchannels. Fig. 8 shows the current signal of the calibration plot (ranging from 10.0 μmol L^{-1} to 80.0 μmol L^{-1}, I (nA)$=-0.15$ (± 0.04)$+0.53$ (± 0.012) [Glucose] (μmol L^{-1}), R^2: 0.995) obtained for glucose analysis, and also for samples after passing through a microreactor with immobilised GOx and finally the signal of samples without contact with immobilised GOx. The last group of measurements is very important to evaluate the signal from other interfering species. These last signals were subtracted from the sample signal in order to obtain the real concentration of glucose.

As shown in Fig. 8, the calibration plot was satisfactory for quantifying glucose in the analysed samples. Table 1 shows the different D-glucose concentration values of samples and their respective RSD, obtained via amperometric and spectrophotometric methods. In order to compare the results, a paired t-test was applied. The obtained value showed no evidence of systematic differences between the two methods ($t_{calculated,\ 0.05,\ 4}=1.35 < t_{tabled,\ 0.05,\ 4}=2.78$).

With regards to the samples' glucose concentration, it is interesting to notice that the ratio of natural to industrial coconut water varied between different brands, reaching concentrations almost 25 times higher for some industrial waters. It is known that the amount of glucose in coconut water varies with maturation and that it is also added to industrialised samples as a way to improve flavour [28,29]. In this way, the proposed methodology can be used to make a rapid investigation of coconut water adulteration.

4. Conclusion

In this study, a new fast, cheap and efficient PMMA surface modification for GOx immobilisation is presented. The developed microchannel presents good long-term stability, showing a signal reduction of 50.0% over one week of intense use. Even so, the remaining activity was sufficient for quantifications of approximately 0.10 mmol L^{-1}, merely requiring a new calibration of the reactor before its utilisation. The methodology for D-glucose determination was applied to coconut water samples, requiring only a few microlitres of each sample (10.0 μL after dilution), allied to a high sample frequency (60 samples h^{-1}) and a significant bioconversion (36.6%), allowing its use for the quality control of such samples. Moreover, this new methodology presents considerable values for Michaelis–Menten parameters, with V_{max} of 449 $\pm$ 47.7 nmol min^{-1} and K_M of 7.79 $\pm$ 0.98 mmol. Low detection and quantification limits (0.50 μmol L^{-1} and 1.66 μmol L^{-1}, respectively) and a wide linear range (from 5.00 μmol L^{-1} to 2.00 mmol L^{-1}) were also found, which are useful characteristics

for quality control analysis. It is important to note that the linear working range can be modified according to operator needs, simply by changing the parameters of analysis (presented in Fig. 5).

Acknowledgements

The authors are grateful for the financial support from Brazilian Foundations (CAPES (Grant no. DS-32005016) and CNPq – Process 306504-2011-1), to the State Foundations (FAPESP and FAPEMIG (Grant no. APQ-OO173-11)) and to the Universities sponsoring programs: NAP-NN (University of Sao Paulo (USP)) and PROPESQ (UFJF).

References

[1] A. Manz, N. Graber, H.M. Widmer, Sens. Actuators B: Chem. 1 (1990) 244–248.
[2] L. Szekely, A. Guttman, Electrophoresis 26 (2005) 4590–4604.
[3] D. Figeys, D. Pinto, Anal. Chem. 72 (2000) 330A–335A.
[4] J. Gao, J.D. Xu, L.E. Locascio, C.S. Lee, Anal. Chem. 73 (2001) 2648–2655.
[5] T. Richter, L.L. Shultz-Lockyear, R.D. Oleschuk, U. Bilitewski, D.J. Harrison, Sens. Actuators B: Chem. 81 (2002) 369–376.
[6] G. Drager, C. Kiss, U. Kunz, A. Kirschning, Org. Biomol. Chem. 5 (2007) 3657–3664.
[7] S. Ekstrom, P. Onnerfjord, J. Nilsson, M. Bengtsson, T. Laurell, G. Marko-Varga, Anal. Chem. 72 (2000) 286–293.
[8] M.S. Thomsen, P. Polt, B. Nidetzky, Chem. Commun. 24 (2007) 2527–2529.
[9] L.M. Cerdeira Ferreira, E.T. da Costa, C.L. do Lago, L. Angnes, Biosens. Bioelectron. 47 (2013) 539–544.
[10] Y. Chen, L.Y. Zhang, G. Chen, Electrophoresis 29 (2008) 1801–1814.
[11] F. Fixe, M. Dufva, P. Telleman, C.B.V. Christensen, Nucleic Acids Res. 32 (2004) 1–8.
[12] V. Bulmus, H. Ayhan, E. Piskin, Chem. Eng. J. 65 (1997) 71–76.
[13] S.A. Soper, A.C. Henry, B. Vaidya, M. Galloway, M. Wabuyele, R.L. McCarley, Anal. Chim. Acta 470 (2002) 87–99.
[14] A.C. Henry, T.J. Tutt, M. Galloway, Y.Y. Davidson, C.S. McWhorter, S.A. Soper, R.L. McCarley, Anal. Chem. 72 (2000) 5331–5337.
[15] L. Brown, T. Koerner, J.H. Horton, R.D. Oleschuk, Lab Chip 6 (2006) 66–73.
[16] Y.L. Bai, C.G. Koh, M. Boreman, Y.J. Juang, I.C. Tang, L.J. Lee, S.T. Yang, Langmuir 22 (2006) 9458–9467.
[17] J.M. Guisan, P. Sabuquillo, R. Fernandez-Lafuente, G. Fernandez-Lorente, C. Mateo, P.J. Halling, D. Kennedy, E. Miyata, D. Re, J. Mol. Catal. B: Enzym. 11 (2001) 817–824.
[18] J.Y. Cheng, C.W. Wei, K.H. Hsu, T.H. Young, Sens. Actuators B: Chem. 99 (2004) 186–196.
[19] R.C. Matos, I.G.R. Gutz, L. Angnes, R.S. Fontenele, J.J. Pedrotti, Quim. Nova 24 (2001) 795–798.
[20] J.J. Pedrotti, L. Angnes, I.G.R. Gutz, Electroanalysis 8 (1996) 673–675.
[21] S. Meites, K. Sanielba, Clin. Chem. 19 (1973) 308–311.
[22] A. Matsushita, Y.Z. Ren, K. Matsukawa, H. Inoue, Y. Minami, I. Noda, Y. Ozaki, Vib. Spectrosc. 24 (2000) 171–180.
[23] B. Karlberg, G.E. Pacey, Techniques and Instrumentation in Analytical Chemistry, Elsevier, New York (1989) 6–28.
[24] R.D. O'Neill, J.P. Lowry, G. Rocchitta, C.P. McMahon, P.A. Serra, Trends Anal. Chem. 27 (2008) 78–88.
[25] T. Laurell, J. Drott, L. Rosengren, Biosens. Bioelectron. 10 (1995) 289–299.
[26] J. Lasch, R. Koelsch, Mol. Cell. Biochem. 2 (1973) 71–77.
[27] W. Zhang, Y. Huang, H. Dai, X. Wang, C. Fan, G. Li, Anal. Biochem. 329 (2004) 85–90.
[28] J.C. Jackson, A. Gordon, G. Wizzard, K. McCook, R. Rolle, J. Sci. Food Agric. 84 (2004) 1049–1052.
[29] H.D.S. Oliveira, C.M.P. de Abreu, C.D. dos Santos, M.D. Cardoso, J.E.C. Teixeira, N.C.C. Guimaraes, Cienc. E Agrotecnologia 27 (2003) 1063–1067.